

Controlled Building Mesoporous MoS₂@MoO₂-Doped Magnetic Carbon Sheets for Superior Potassium Ion Storage

Yuting Liu^{a,b,1}, Yaoyao Xiao^{a,b,1}, Fusheng Liu^{a,b}, Pinyu Han^{a,b}, Guohui Qin^{a,b*}

^a *State Key Laboratory Base for Eco-Chemical Engineering, College of Chemical Engineering, Qingdao University of Science and Technology, Qingdao 266042, Shandong, China*

^b *Shandong Collaborative Innovation Center of Eco-Chemical Engineering, Qingdao 266042, Shandong, China*

¹ These authors contribute equally to this work.

Corresponding author.

E-mail address: guohuiq163@sina.com

Directory of contents

Fig. S1 XPS spectrum of N for MoS₂@MoO₂@Fe@CN.

Fig. S2 FESEM images of MoS₂@MoO₂@Fe@CN at various time intervals: (A) 1 h, (B) 2 h, (C) 5 h and (D) 18 h.

Fig. S3 The TEM image of products changing the original agent to (a) pure water. (b) In the absence of Fe. (c) In the absence of CN.

Fig. S4 The XRD curves of (a) taking samples at 2 h, (b) 5 h. (c) The XPS spectrum of the products in the absence of CN. (d) The XRD curve of the products at 120°C.

Fig. S5 (a) N₂ adsorption and desorption isotherm and (b) pore size distribution of MoS₂ based composites.

Fig. S6 XRD patterns of the pristine MoS₂ based electrode and MoS₂ based composite electrode with different discharge/charge depths (the peak signals of MoO₂ were omitted).

Fig. S7 Cross-sectional SEM images of MoS₂@MoO₂@Fe@CN (a) before and (b) after 100 cycles, cross-sectional SEM images of MoS₂@Fe@CN sample (c) before and (d) after 100 cycles at 100 mA g⁻¹. (e) The SEM images of (e) MoS₂@MoO₂@Fe@CN (f) MoS₂@Fe@CN after 500 cycles at 500 mA g⁻¹.

Fig. S8 (a) Nyquist plot after ten cycles of plating stripping and long-term cycling and voltage hysteresis of symmetrical cells at 1 mA cm⁻², respectively. (b) The Nyquist plots of MoS₂ based composite after 500 cycles at 500 mA g⁻¹.

Fig. S9 (a) CV curves of MoS₂@Fe@CN at various scan. (b) b-value determination for MoS₂@Fe@CN at various scan.

Fig. S10 CV profiles of capacitive contribution at scan rates from 0.1 to 2 mV/s (a-e). (f) Specific capacities generated from battery contribution and capacitive contribution at different scan rates for MoS₂@MoO₂@Fe@CN.

Table S1 The comparison of the potassium storage properties between MoS₂@MoO₂@Fe@CN and the previously reported anode materials.

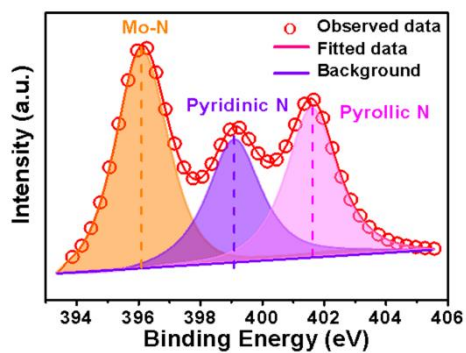


Fig. S1 XPS spectrum of N for MoS₂@MoO₂@Fe@CN.

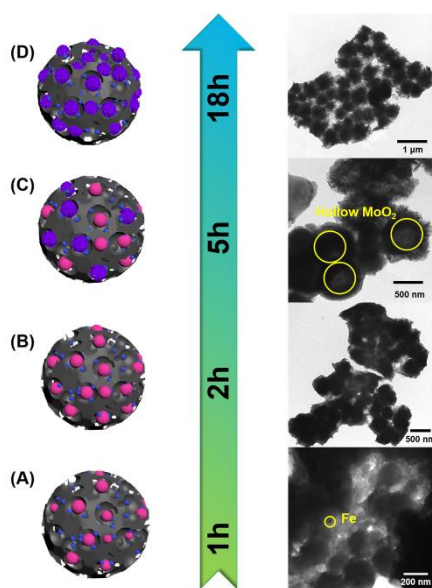


Fig. S2 FESEM images of MoS₂@MoO₂@Fe@CN at various time intervals: (A) 1 h, (B) 2 h, (C) 5 h and (D) 18 h.

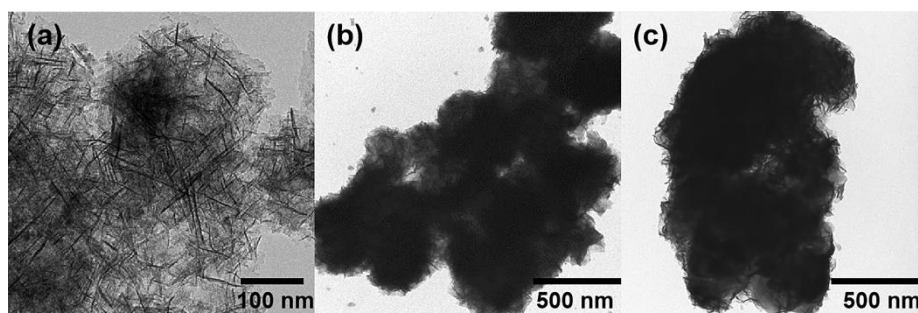


Fig. S3 The TEM image of products changing the original agent to (a) pure water. (b) In the absent of Fe. (c) In the absence of CN.

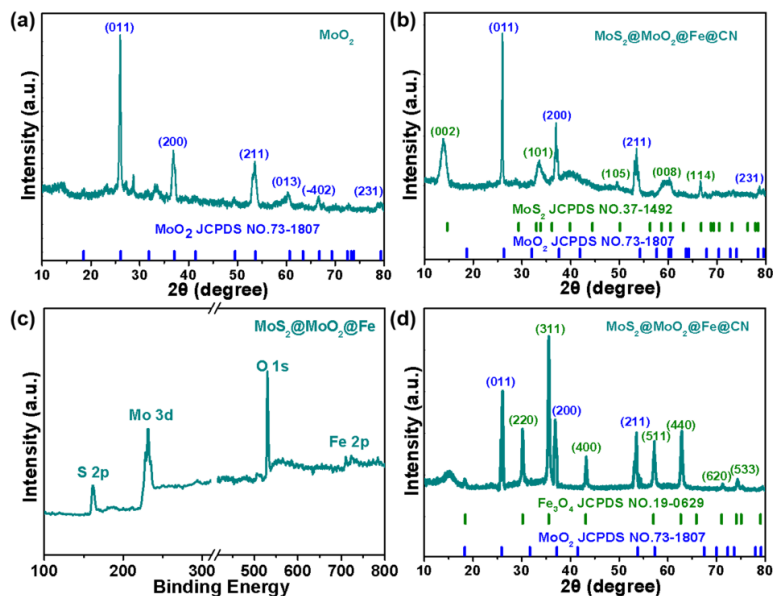


Fig. S4 The XRD curves of (a) taking samples at 2 h. (b) 5 h. (c) The XPS spectrum of the products in the absence of CN. (d) The XRD curve of the products at 120°C.

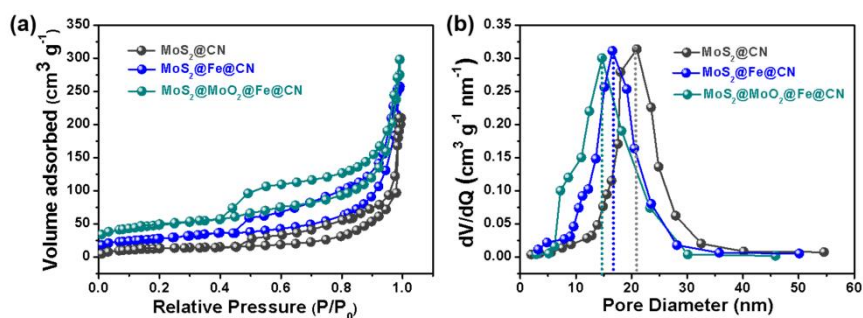


Fig. S5 (a) N_2 adsorption and desorption isotherm and (b) pore size distribution of MoS_2 based composites.

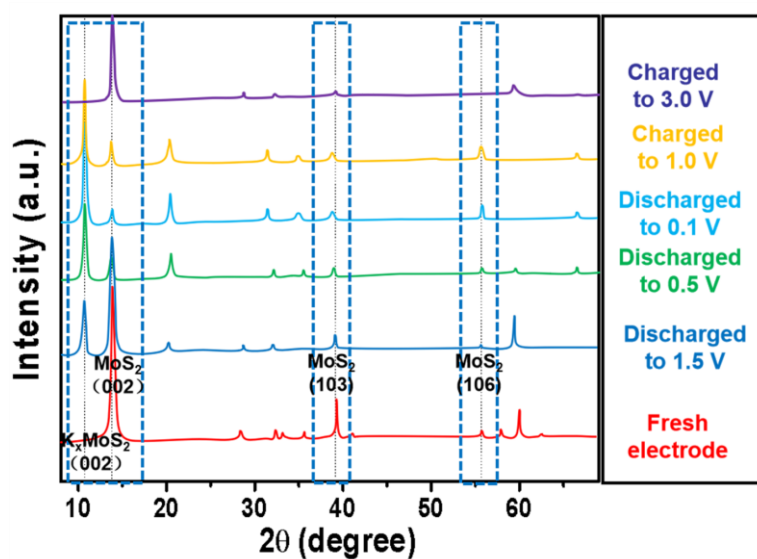


Fig. S6 XRD patterns of the pristine MoS_2 based electrode and MoS_2 based composite electrode with different discharge/charge depths (the peak signals of MoO_2 were omitted).

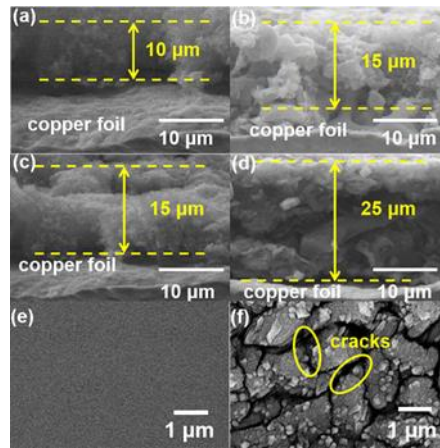


Fig. S7 Cross-sectional SEM images of $\text{MoS}_2@\text{MoO}_2@\text{Fe}@\text{CN}$ (a) before and (b) after 100 cycles, cross-sectional SEM images of $\text{MoS}_2@\text{Fe}@\text{CN}$ sample (c) before and (d) after 100 cycles at 100 mA g^{-1} . (e) The SEM images of (e) $\text{MoS}_2@\text{MoO}_2@\text{Fe}@\text{CN}$ (f) $\text{MoS}_2@\text{Fe}@\text{CN}$ after 500 cycles at 500 mA g^{-1} .

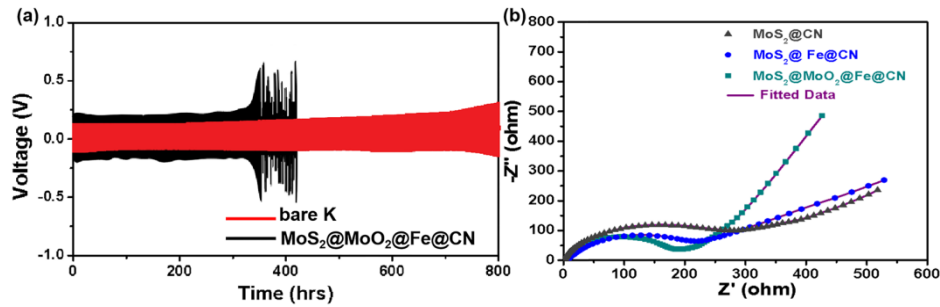


Fig. S8 (a) Nyquist plot after ten cycles of plating stripping and long-term cycling and voltage hysteresis of symmetrical cells at 1 mA cm^{-2} , respectively. (b) The Nyquist plots of MoS_2 based composite after 500 cycles at 500 mA g^{-1} .

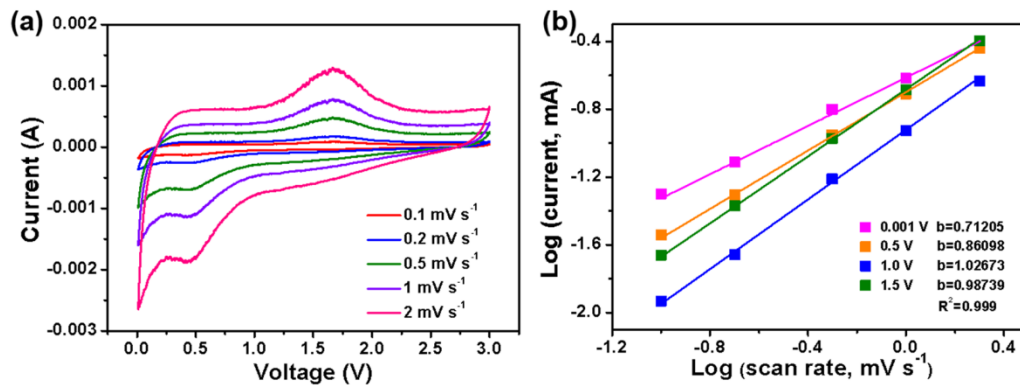


Fig. S9 (a) CV curves of $\text{MoS}_2@\text{Fe}@\text{CN}$ at various scan. (b) b-value determination for $\text{MoS}_2@\text{Fe}@\text{CN}$ at various scan.

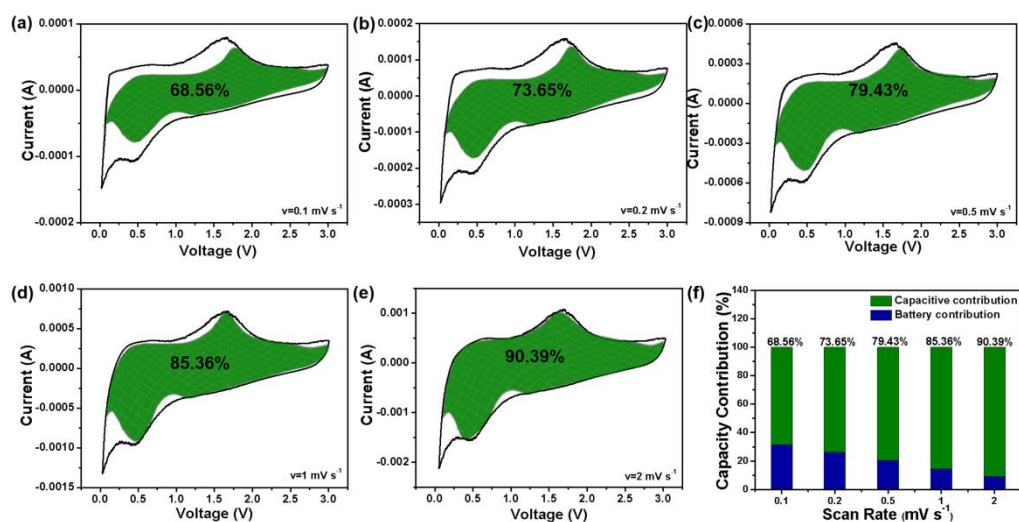


Fig. S10 CV profiles of capacitive contribution at scan rates from 0.1 to 2 mV/s (a-e). (f) Specific capacities generated from battery contribution and capacitive contribution at different scan rates for MoS₂@MoO₂@Fe@CN.

Table S1 The comparison of the potassium storage properties between MoS₂@MoO₂@Fe@CN and the previously reported anode materials.

Materials	Current density (mA g ⁻¹)	Cycle number	Capacity (mAh g ⁻¹)	Reference
D-MoS ₂	50	1	104	40
	100	100	94	
MoS ₂ NFs	50	1	77	
	100	100	67	
Sn ₄ P ₃ @C	50	50	307.2	41
Ordered mesoporous carbon	50	100	257.4	42
K ₄ PTC@CNT	50	500	132	43
MoS ₂ @SnO ₂ @C	100	25	250	44
MoS ₂ @MoO ₂ @Fe@CN	50	1	351	This work
	100	100	312	
	500	500	271	